J. Electrochem. Sci. Eng. **16** (2026) 3422; https://doi.org/10.5599/jese.3422

Open Access : : ISSN 1847-9286
https://pub.iapchem.org/ojs/index.php/JESE

Original scientific paper

Modified carbon paste electrode as a sensitive electrochemical sensor for quantification of chemotherapy drug imatinib

Dhay S. Naji[1], Ahmed Hameed AlSaeedi[2,✉], Emad Salaam Abood[3] and Karrar M. Obaid[4]

[1]*Department of Chemical Engineering, College of Engineering, University of Babylon, Iraq*
[2]*Faculty of Pharmacy, Department of Pharmaceutics, University of Hilla, Babylon, Iraq*
[3]*Medical Physics Department, College of Science, University of Hilla, Babylon, Iraq*
[4]*BioChemistry Department, College of Science, Al-Mustaqbal University, Hilla, Iraq*

Corresponding Author: ✉ahmed.alsaeedi@outlook.de

Received: April 15, 2026; Accepted: June 1, 2026; Published: June 10, 2026

Abstract

The preferred tyrosine kinase inhibitor for treating gastrointestinal stromal tumours and chronic myeloid leukaemia is imatinib (IMT). Nevertheless, IMT has disadvantages, including resistance to the medication and notable variations in pharmacokinetics among patients. To address this problem, an analytical procedure for IMT determination was developed that incorporated $MnMoO_4$@multi-walled carbon nanotubes (MWCNTs) into a carbon paste electrode (CPE) matrix to create an electrochemical sensing platform, $MnMoO_4$@MWCNT/CPE. A hydrothermal technique was used to synthesize $MnMoO_4$@MWCNT. Under carefully adjusted conditions, electrochemical characterization using differential pulse voltammetry showed a concentration interval with a linear response for IMT between 0.01 and 120.0 µM. In addition to a significant sensitivity of 0.3508 µA μM^{-1}, quantitative analysis yielded detection and quantification limits of 3 and 7 nM. The developed electrochemical probe demonstrated outstanding analytical performance, high stability, and repeatability when used to quantify IMT in pharmaceutical product samples.

Keywords

Cancer treatment; 2-phenylaminopyrimidine derivative; electrochemical monitoring; bimetallic oxide; carbon nanostructure; pharmaceutical tablets

Introduction

Imatinib (IMT), known under the brand name Gleevec, is a chemotherapeutic medication used to treat some types of cancer. In 2001, Food and Drug Administration (FDA) approved this medication for use in the treatment of various malignancies in the United States [1]. IMT decreases cell proliferation or apoptosis in certain cancer cells by blocking the action of a synthetic tyrosine kinase,

a synthetic tyrosine kinase, which was designed to target the Bcr-Abl fusion protein. IMT is an anti-cancer medication that is used specifically to destroy cancer cells rather than harm them through rapid cell division. Additionally, there might be a connection between the clinical response and the IMT concentration. Because levels may be insufficient due to a significant chemical reaction or a complete cytotoxic response, low plasma IMT concentrations may suggest an ineffective medication [2]. As a result, monitoring IMT levels in actual biological samples is crucial for clinical diagnosis [3].

IMT analysis has already been conducted using a variety of analytical techniques, including capillary electrophoresis (CE) [4], ultra-performance liquid chromatography (UPLC) [5], high-performance liquid chromatography (HPLC) [6] and fluorescence [7]. The electrochemical method has also been proposed for this drug detection due to the electroactive spots on the IMB surface. To assess lower IMT quantities, it is difficult to choose a method that is sensitive and efficient in detection while keeping at the same time low operational expenses. To date, several electrochemical studies have been conducted using electrochemical sensors [8,9].

Because of their many advantages, including a straightforward fabrication process, low cost, easy surface regeneration, minimal background current, and significant miniaturization capability, carbon paste electrodes (CPEs) are widely recognized as one of the most favoured types of working electrodes in electrochemical research [10]. Nevertheless, a significant drawback of bare CPEs is their poor electrochemical performance, primarily due to inadequate electron transfer at the electrode/electrolyte interface. Chemically modified electrodes (CMEs) have been used as a workable solution to this problem [11]. It has been shown that adding several modifiers, including nanostructures, conductive polymers, and biomolecules, greatly improves the electrochemical characteristics of CPEs. These changes enhance electron-transfer kinetics, thereby raising the sensitivity and selectivity for specific analytes. As a result, these developments expand the use of CPEs in electrochemical sensing and analytical methods, making them a flexible platform for creative study in this field. The use of various nanostructured materials as active electrocatalysts has recently emerged as a promising approach to improve the performance of electrochemical sensors, with carbon-based nanomaterials receiving considerable attention due to their low cost, remarkable sensitivity, and ease of production [12].

The remarkable magnetic, optical, and electrical characteristics and environmental safety [13] of bimetal oxide compounds have garnered significant interest in recent studies. Because the two metals work in concert, bimetal oxides have superior characteristics over monometal oxides [13]. Additionally, bimetallic oxides ABO_4, including $MgCo_2O_4$, $ZnCo_2O_4$ and $CuCo_2O_4$, have shown remarkable catalytic, mechanical, and electrical properties, as well as outstanding chemical and thermal stability [14,15].

High surface area, multiple oxidation states, high stability, and reversible reduction (Mn^{4+} to Mn^{3+}) are among the beneficial physicochemical characteristics of manganese oxide. Metal oxides doped with high-valent metals, including Mo, have been used recently to improve the electrocatalytic activity of catalysts by adjusting their energy levels [16]. Owing to their electrical characteristics, high surface charge, and strong electrocatalytic activity, molybdenum oxides receive consideration as electrode materials [16]. Furthermore, molybdenum oxide has a wide band gap (>2.7 eV) and can function as a p-type semiconductor due to its multiple oxidation states, ranging from Mo^{2+} to Mo^{6+} [17]. MoO_3 is used in a number of applications, including superconductors, energy storage devices, thermal materials, medical devices [17], and electrochemical sensors, owing to its unique properties. Molybdates are used in a wide range of applications, including energy storage, luminescent characteristics, heavy metal detection sensors, supercapacitors [18] and hybrid systems.

(cc) BY

Among many transition metal oxides, Mn and Mo oxides have great electrocatalytic behaviour. Furthermore, efficient interaction with the target analyte is enabled by the different oxidation states and the polarity of rapidly moving electrons [19]. On the other hand, $MnMoO_4$ (MMO) has very low electrical conductivity [19], which could affect electrochemical performance. MMOs are frequently encapsulated in carbon-based materials, such as conducting polymers, carbon nanofibers, carbon nanotubes, and graphene oxides, to overcome this challenge and enhance their electrocatalytic activity [19].

One of the most promising options for creating composites based on bimetal oxide compounds is carbon nanostructures, such as carbon nanotubes (CNTs) [20]. Significant electrical conductivity, a large active surface area, outstanding strength, and chemical inertness are all features of CNTs. Because of these benefits, integrating CNTs with bimetal oxide compounds to improve their electrochemical performance is very appealing [21]. It is anticipated that bimetallic oxide compounds and multi-walled carbon nanotube (MWCNT)- based nanocomposites will demonstrate synergistic effects that enhance electrochemical sensing efficiency while retaining the benefits of each component [22].

In this work, we offer an appropriate voltammetric technique for determining IMT utilizing $MnMoO_4$@MWCNT/CPE. Because $MnMoO_4$ and MWCNTs work well together, the $MnMoO_4$@ @MWCNT/CPE performs well for IMT determination. Additionally, the as-developed $MnMoO_4$@ @MWCNT/CPE sensing device demonstrated high sensitivity for IMT assessment. To investigate its practical applicability, the sensing platform is also used to measure IMT in IMT pharmaceutical tablets.

Experimental

Chemicals and apparatus

Chemicals, including IMT, MWCNTs, HNO_3, H_2SO_4, $Na_2MoO_4{\cdot}2H_2O$, ethylene glycol (EG), $Mn(NO_3)_2{\cdot}4H_2O$, and poly(ethylene glycol), were purchased from Sigma-Aldrich and Merck and were used without further purification in their original form. IMT tablets (400 mg per tablet) were purchased from the DailyMed company (USA). The electrochemical apparatus (PGSTAT 302N Potentiostat/galvanostat, Metrohm, The Netherlands) was used for the determination of IMT. The working electrodes (WEs), counter electrode (CE) and reference electrode (RE) in a three-electrode cell were unmodified CPE or $MnMoO_4$@MWCNT/CPE, platinum wire, and Ag/AgCl (inner solution: KCl 3.0 M), respectively. 0.1 M phosphate buffer (PB) solution was used as the supporting electrolyte.

Electrochemical methodology

Cyclic voltammetry (CV) was performed in the potential range of 0.4 to 0.91 V *vs.* Ag/AgCl at a scan rate of 50 mV s^{-1}. The oxidation mechanism of IMT was examined at the surface of an unmodified CPE and $MnMoO_4$@MWCNT/CPE. The differential pulse voltammetry (DPV) measurements to determine IMT were recorded on the $MnMoO_4$@MWCNT/CPE surface from 0.44 to 0.8 V with a step potential of 0.01 V, a pulse amplitude of 0.025 V, and a scan rate of 50 mV s^{-1}.

Synthesis of $MnMoO_4$@MWCNT composite

The standard $MnMoO_4$@MWCNT composite procedure requires refluxing raw MWCNTs in a 100 ml HNO_3/H_2SO_4 mixture containing 8 M of each acid at 80 °C for 4 hours. The acid-treated MWCNTs were centrifuged, then cleaned multiple times with ethanol and distilled (DI) water, and

finally dried at 95 °C for 1 night. The dissolution of 1.20 g of $Na_2MoO_4{\cdot}2H_2O$ required 20 ml of ethylene glycol (EG). The dissolution of 1.25 grams of $Mn(NO_3)_2{\cdot}4H_2O$ required 20 milliliters of EG, which was prepared separately. The two solutions were mixed and stirred continuously for 35 minutes, resulting in a clear solution. The mixing process began after they were combined and continued for 30 minutes. The addition of 1.0 mL of poly(ethylene glycol) was performed while the solution was stirred continuously. The mixture received 0.0245 g of acid-treated MWCNTs, corresponding to 1 weight percent of the metal precursor. The completed solution was placed in a Teflon-lined stainless-steel autoclave with a capacity of 100 cm^3. The autoclave was moved to an oven maintained at 170 °C for 12 hours. The autoclave needs to reach ambient temperature after that. Centrifugation was used to separate the precipitate, which was then washed with ethanol and DI water, followed by drying for 4 h at 100 °C. The same procedure for synthesizing bare $MnMoO_4$ was performed without acid-treated MWCNTs.

Preparation of $MnMoO_4$@MWCNT/CPE

Graphite powder (196.0 mg) was combined with 4.0 milligrams of $MnMoO_4$@MWCNT and the appropriate amount of paraffin oil to produce the $MnMoO_4$@MWCNT/CPE sensor, which was prepared by hand mixing in a mortar with a pestle. A copper wire was inserted into the rear portion of the paste before compacting a portion of the mixture into a glass holder with a tubular design. The carbon paste surface was treated with soft paper to smooth its surface. The scraping was used to remove material from the electrode surface.

Electroactive surface area (A) of unmodified CPE and $MnMoO_4$@MWCNT/CPE was evaluated using $[Fe(CN)_6]^{3-/4-}$ as a redox probe by CV. The CV responses of bare CPE and $MnMoO_4$@MWCNT/ /CPE were recorded in 0.1 M KCl solution in the presence of 5.0 mM $[Fe(CN)_6]^{3-/4-}$ as a redox probe. At the surface of $MnMoO_4$@MWCNT/CPE, a decrease in ΔE_p and an increase in the values of the redox peak currents of the redox probe were observed compared to bare CPE. These observations can be attributed to faster electron-transfer kinetics and a higher electroactive surface area of $MnMoO_4$@MWCNT/CPE. To verify this, the electroactive surface areas of the bare CPE and $MnMoO_4$@MWCNT/CPE were determined using the Randles-Ševčik Equation (1):

$$I_p = (2.69\times10^5)n^{3/2}AD^{1/2}\nu^{1/2}C \quad (1)$$

where I_p presents the peak current, n is the number of electrons participating in the redox process (n = 1), A presents the electroactive surface area of the electrode, D is the diffusion coefficient (7.6×10^{-6} cm^2 s^{-1}), ν represents the scan rate (0.1 V s^{-1}) and C is the concentration of redox probe. The corresponding values of active surface area of $MnMoO_4$@MWCNT/CPE and bare CPE were, after using Equation (1), determined to be 0.25 and 0.095 cm^2, respectively.

Results and discussion

Electrochemical behaviour of IMT on different electrodes

The study assessed how pH in the range 3.0 to 9.0 in 0.1 M PB affected IMT measurements using DPV at $MnMoO_4$@MWCNT/CPE. The DPV results show that the anodic peak current (I_{pa}) of IMT varies with pH and reaches its maximum at neutral pH. The I_{pa} of IMT determination begins to decrease at pH 7.0 and continues until pH 9.0. The ideal pH for measuring IMT at the $MnMoO_4$@MWCNT/CPE in 0.1 M PBS is therefore 7.0.

CV tests were conducted to study the mechanism of electrochemical oxidation of IMT. Figure 1 shows the recorded cyclic voltammograms of $MnMoO_4$@MWCNT/CPE and unmodified CPE in

(cc) BY

0.1 M PB, pH 7.0, containing 30.0 µM IMT. The electrochemical processes exhibited an irreversible oxidation peak, corresponding to the IMT oxidation reaction, as shown in Figure 1. The unmodified CPE produces a lower peak current occurring at a more positive potential (730 mV). The CPE peak current of IMT oxidation shows an increase to 11.0 µA at $MnMoO_4$@MWCNT/CPE and the current peak potential shifts to 640 mV. Therefore, $MnMoO_4$@MWCNT/CPE demonstrates better electrocatalytic performance for IMT oxidation than pure CPE.

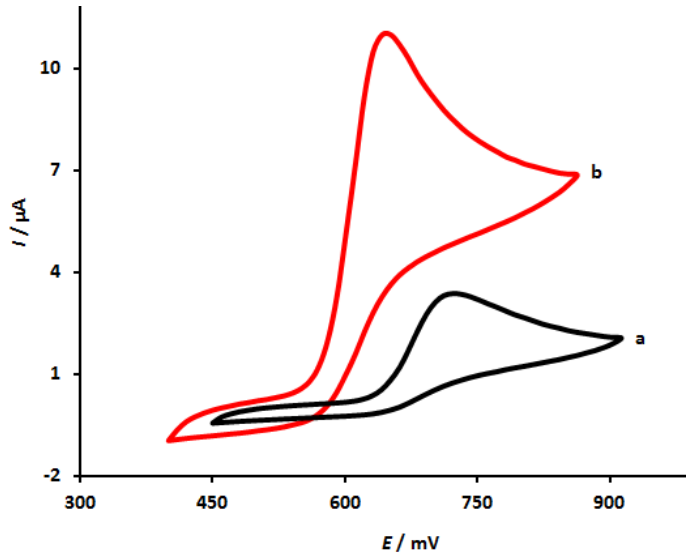

Figure 1. *CV response of unmodified CPE (a) and $MnMoO_4$@MWCNT/CPE (b) in 0.1 M PB, pH 7.0 containing 30.0 µM IMT, at a scan rate of 50 mV s^{-1}*

Influence of scan rate on the electrochemical behaviour of IMT at $MnMoO_4$@MWCNT/CPE

As shown in Figure 2A, the CV responses of $MnMoO_4$@MWCNT/CPE were collected at different scan rates in 0.1 M PB, pH 7.0, containing 30.0 µM IMT, to ascertain the mechanism of electrochemical oxidation of IMT. The CV responses show that as the scan rate increases, the peak currents of IMT oxidation increase. Additionally, the square root of scan rate ($\nu^{1/2}$) determines the peak currents of IMT oxidation in a linear fashion ($I_{pa} = 1.4664\,\nu^{1/2} + 0.4435$, $R^2 = 0.9997$) (Figure 2B). The study's findings demonstrate that the electrochemical oxidation of IMT at the $MnMoO_4$@MWCNT/CPE is diffusion-controlled.

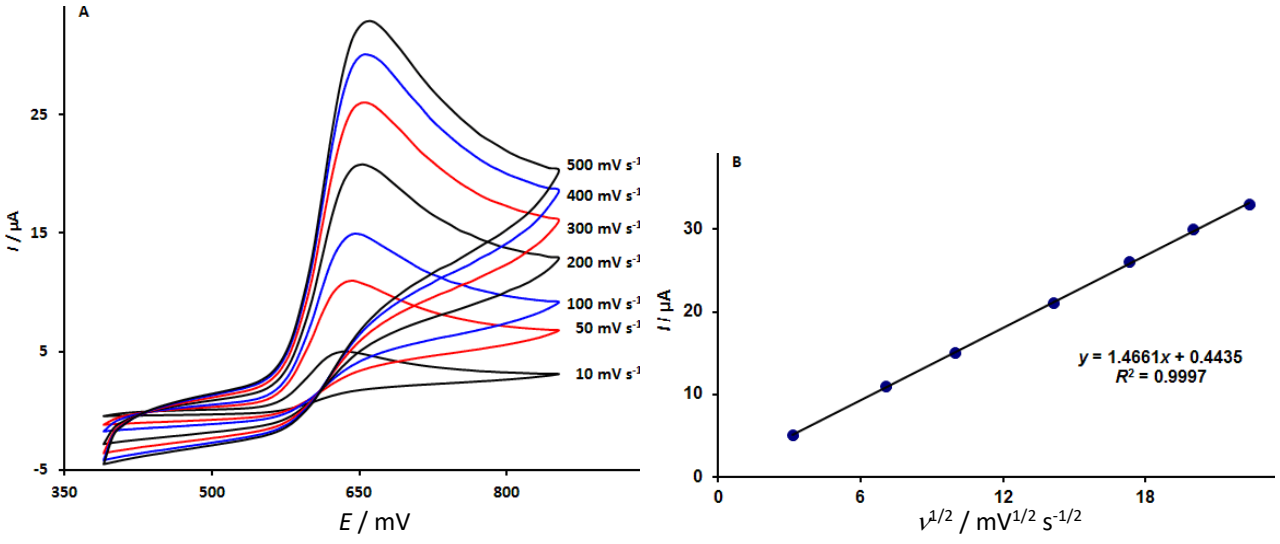

Figure 2. *(A) CV responses of $MnMoO_4$@MWCNT/CPE in 0.1 M PB, pH 7.0 containing 30.0 µM IMT at various scan rates, (B) a linear graph depicting the peak currents of IMT oxidation plotted* vs. $\nu^{1/2}$

Chronoamperometric studies

As shown in Figure 3, chronoamperograms were recorded at the MnMoO4@MWCNT/CPE in 0.1 M PBS (pH 7.0) containing IMT at different concentrations to assess the diffusion coefficient of IMT.

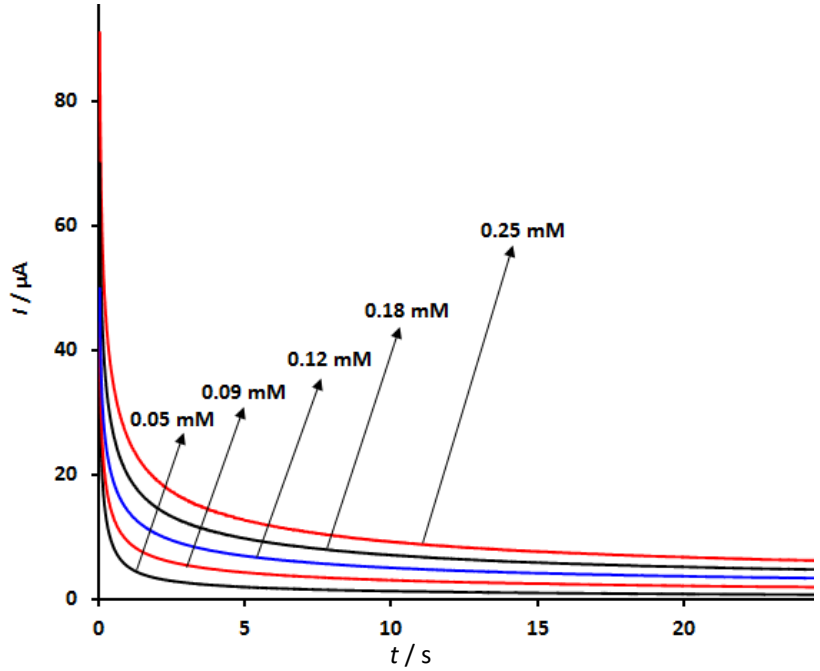

Figure 3. *The chronoamperometric responses of $MnMoO_4$@MWCNT/CPE in 0.1 M PB, pH 7.0, at varying doses of IMT (0.05 to 0.25 mM) (step potential: 0.69 V)*

To estimate the diffusion coefficient from chronoamperometric experiments, the Cottrell Equation (2) was used:

$$I = nFAD^{1/2}C/(\pi t)^{1/2} \quad (2)$$

where I / A stands for current, n for the number of electrons transferred in the oxidation reaction, F for Faraday's constant (96485 C mol^{-1}), A / cm^2 for electrode area, D / cm^2 s^{-1} for diffusion coefficient, C / mol cm^{-3} for electroactive compound concentration, and t /s for time. The Cottrell equation revealed that the currents were linearly related to $t^{-1/2}$ (Cottrell plots, Figure 4A) from the chronoamperograms recorded at each concentration. Additionally, a linear correlation between the IMT concentration and slopes of Cottrell plots was observed (Figure 4B). The diffusion coefficient was therefore calculated to be 2.7×10^{-5} cm^2 s^{-1}.

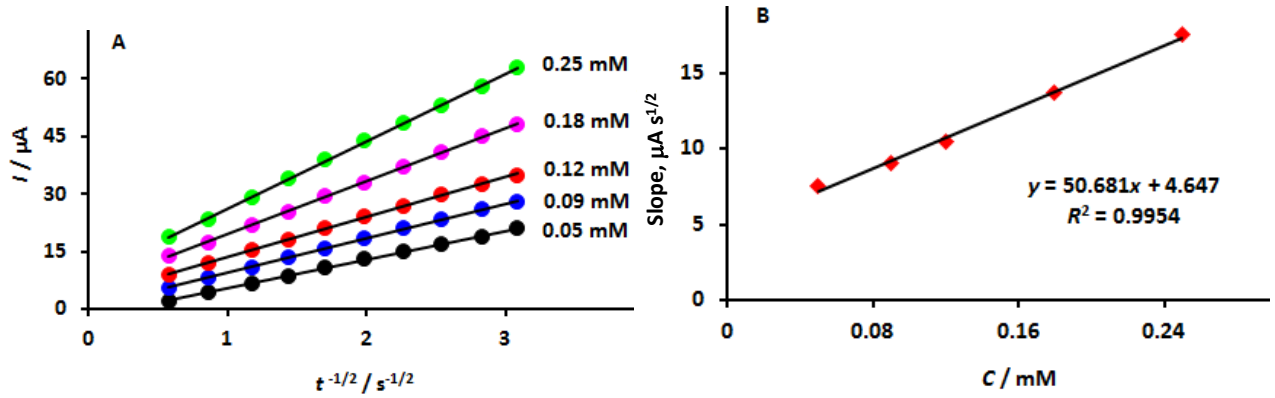

Figure 4. *(A) Cottrell plots derived from chronoamperograms collected for each IMT concentration and (B) a linear plot showing slopes of Cottrell plots versus IMT concentrations*

(cc) BY

DPV measurements of various concentrations of IMT at the $MnMoO_4$@MWCNT/CPE

IMT was quantitatively measured using differential pulse voltammetry (DPV), a sensitive voltammetric technique (Figure 5). The peak oxidation currents increase with increasing IMT concentration, and the related calibration plot is shown in Figure 6.

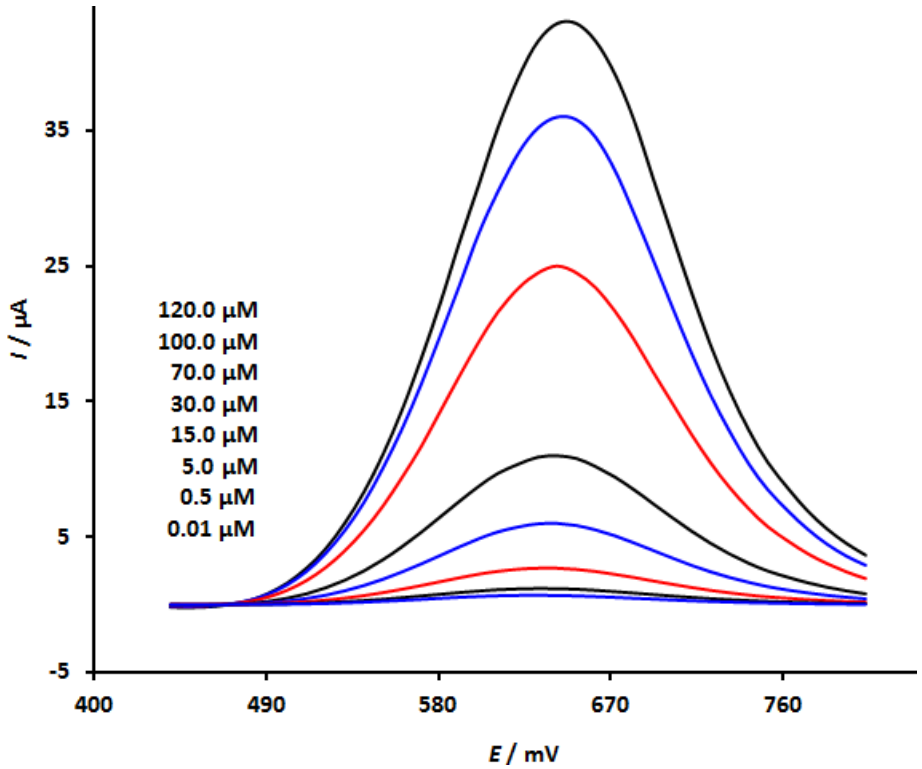

Figure 5. *DPV responses of $MnMoO_4$@MWCNT/CPE in 0.1 M PB, pH 7.0, containing IMT at various concentrations (0.01 to 120.0 µM) under the optimized conditions*

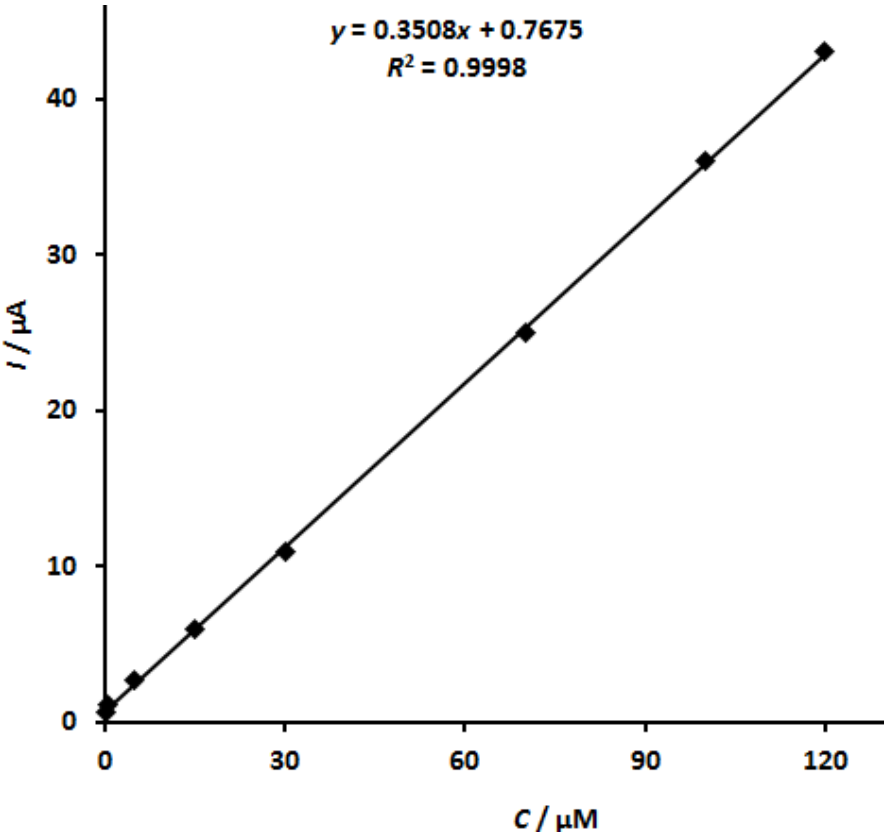

Figure 6. *A linear graph depicting the peak currents of IMT oxidation plotted vs. concentrations*

As the IMT concentration was raised from 0.01 μM to 120.0 μM, the DPV responses increased linearly. I_{pa} = 0.3508 C_{IMT} + 0.97675 (R^2 = 0.9998) is the fitting equation that was obtained. Sensitivity was obtained as 0.3508 μA μM^{-1} and the limit of detection (LOD) can be determined using Equation (3):

$$LOD = 3S_{Blank}/m \quad (3)$$

In this case, m denotes the slope obtained from the calibration plot, and S_{Blank} is the standard deviation of 12 blank data without IMT. LOD was determined to be 0.003 μM.
Also, the limit of quantification (LOQ) using LOD = $10S_{Blank}/m$ was calculated as 0.007 μM.

Stability, reproducibility, and repeatability studies of $MnMoO_4$@MWCNT/CPE -based sensor for the determination of IMT

During continuous operation over various time periods, the stability of the $MnMoO_4$@MWCNT/CPE-based sensor was assessed. To track changes in the sensor's performance, the response was recorded at regular intervals in 0.1 M PB (pH 7.0) containing 40.0 μM IMT. After 20 days of storage at room temperature, 97.8 % of the initial current response to IMT was retained, indicating good stability of the $MnMoO_4$@MWCNT/CPE sensing platform. Five electrodes ($MnMoO_4$@MWCNT/CPE) prepared using the same techniques were evaluated for repeatability, and their DPV responses were recorded in 0.1 M PBS (pH 7.0) containing 40.0 μM IMT. Their responses were consistent, with a 4.0 % relative standard deviation (RSD). Additionally, the $MnMoO_4$@MWCNT/CPE-based sensor was used to measure 40.0 μM IMT in 0.1 M PB with pH 7.0 during seven experiments. The results showed good reproducibility in IMT determination, with an RSD of 2.3 % (n = 7).

Applicability of the $MnMoO_4$@MWCNT/CPE sensing platform for real sample analysis

Additionally, a study was conducted to demonstrate the suitability of the $MnMoO_4$@MWCNT/CPE sensing platform for determining IMT in IMT pharmaceutical tablets. The IMT tablets were utilized to analyse actual samples for this purpose. First, the processed samples were examined using DPV measurements, and the resulting current response was used to calculate the IMT concentrations. The materials produced were then mixed with specific IMT concentrations, and recovery studies were conducted to determine the IMT. The calibration plot was used to determine the amounts found in recovery experiments. Table 1 summarizes the findings. The $MnMoO_4$@MWCNT/CPE sensing platform yields recoveries of 96.9 to 103.6 % and RSDs of 1.9 to 3.3 %, indicating good applicability for determining IMT in actual samples.

Table 1. *Results of IMT determination in tablet samples using $MnMoO_4$@MWCNT/CPE sensing platform (n = 5)*

Sample	Concentrations of IMT, μM		Recovery, %	RSD, %
	Added	Found		
IMT tablet	0	2.4	-	3.3
	3.0	5.5	101.8	1.9
	4.0	6.2	96.9	2.2
	5.0	7.3	98.6	2.7
	6.0	8.7	103.6	2.4

Conclusion

The solvothermal approach was used in this work to readily synthesize the $MnMoO_4$@MWCNT nanostructure. As anticipated, the $MnMoO_4$@MWCNT/CPE sensing platform exhibited a markedly enhanced oxidation peak current for IMT at reduced overpotentials compared to pure CPE. According to the DPV measurements, the oxidation peak currents showed a linear dependence on

(cc) BY

IMT concentrations between 0.01 and 120.0 µM, with a limit of detection of 0.003 µM. Ultimately, the developed voltammetric method was successfully used to determine IMT in tablet samples with good recoveries.

Funding: *Not applicable.*

References

[1] M. Habeck, FDA licences imatinib mesylate for CML, *The Lancet Oncology* **3** (2002) 6. https://doi.org/10.1016/S1470-2045(01)00608-8

[2] M. Saeed, G. Gupta, M. A. Abourehab, P. Kesharwani, Redefining cancer treatment: the role of imatinib nanoparticles in precision medicine, *International Journal of Pharmaceutics* **683** (2025) 126027. https://doi.org/10.1016/j.ijpharm.2025.126027

[3] K. Mioduszewska, J. Dołżonek, D. Wyrzykowski, Ł. Kubik, P. Wiczling, C. Sikorska, M. Toński, Z. Kaczyński, P. Stepnowski, A. Białk-Bielińska, Overview of experimental and computational methods for the determination of the pKa values of 5-fluorouracil, cyclophosphamide, ifosfamide, imatinib and methotrexate, *TrAC Trends in Analytical Chemistry* **97** (2017) 283-296. https://doi.org/10.1016/j.trac.2017.09.009

[4] M. Forough, K. Farhadi, A. Eyshi, R. Molaei, H. Khalili, V. J. Kouzegaran, A.A. Matin, Rapid ionic liquid-supported nano-hybrid composite reinforced hollow-fiber electromembrane extraction followed by field-amplified sample injection-capillary electrophoresis: an effective approach for extraction and quantification of Imatinib mesylate in human plasma, *Journal of Chromatography A* **1516** (2017) 21-34. https://doi.org/10.1016/j.chroma.2017.08.017

[5] C. Qi, Q. Cai, P. Zhao, X. Jia, N. Lu, L. He, X. Hou, The metal-organic framework MIL-101 (Cr) as efficient adsorbent in a vortex-assisted dispersive solid-phase extraction of imatinib mesylate in rat plasma coupled with ultra-performance liquid chromatography/mass spectrometry: Application to a pharmacokinetic study, *Journal of Chromatography A* **1449** (2016) 30-38. https://doi.org/10.1016/j.chroma.2016.04.055

[6] J. F. Jourdil, J. Tonini, F. Stanke-Labesque, Simultaneous quantitation of azole antifungals, antibiotics, imatinib, and raltegravir in human plasma by two-dimensional high-performance liquid chromatography–tandem mass spectrometry, *Journal of Chromatography B* **919** (2013) 1-9. https://doi.org/10.1016/j.jchromb.2012.12.028

[7] E. A. Afshar, M. A. Taher, Z. Hashisho, H. Karimi-Maleh, S. Rajendran, Y. Vasseghian, Determination and measurement of Imatinib by a fluorescence quenching sensor based on halloysite nanotubes modified by zirconium metal organic framework, *Materials Chemistry and Physics* **295** (2023) 127157. https://doi.org/10.1016/j.matchemphys.2022.127157

[8] Y. Chen, Z. Liu, D. Bai, Determination of imatinib as anticancer drug in serum and urine samples by electrochemical technique using a chitosan/graphene oxide modified electrode, *Alexandria Engineering Journal* **93** (2024) 80-89. https://doi.org/10.1016/j.aej.2024.03.001

[9] J. Rodríguez, G. Castañeda, I. Lizcano, Electrochemical sensor for leukemia drug imatinib determination in urine by adsorptive striping square wave voltammetry using modified screen-printed electrodes, *Electrochimica Acta* **269** (2018) 668-675. https://doi.org/10.1016/j.electacta.2018.03.051

[10] M. Achache, S. El Boumlasy, D. Bouchta, M. Choukairi, Development and applications of carbon paste and Sonogel-Carbon electrodes modified with nanomaterials: Perspectives in pharmaceutical, biological, environmental and food analysis: A review, *TrAC Trends in Analytical Chemistry* **194** (2025) 118502. https://doi.org/10.1016/j.trac.2025.118502

[11] Y. Yu, M. T. Hoang, Y. Yang, H. Wang, Critical assessment of carbon pastes for carbon electrode-based perovskite solar cells, *Carbon* **205** (2023) 270-293. https://doi.org/10.1016/j.carbon.2023.01.046

[12] A. Ourari, B. Ketfi, S. I. Malha, A. Amine, Electrocatalytic reduction of nitrite and bromate and their highly sensitive determination on carbon paste electrode modified with new copper Schiff base complex, *Journal of Electroanalytical Chemistry* **797** (2017) 31-36. https://doi.org/10.1016/j.jelechem.2017.04.046

[13] G. S. Sree, K.V. Ranjitha, B. J. Reddy, B. S. Mohan, C. R. Kant, Fabrication of RGO based bimetal oxides ternary composite for deterioration of handloom dye and pathogens from polluted water, *Inorganic Chemistry Communications* **155** (2023) 111054. https://doi.org/10.1016/j.inoche.2023.111054

[14] S. R. Jamnani, A. Rezapour, A. B. Khatibani, E. B. Tochaee, A. Azadbar, The effect of graphene on sensing behavior of hydrothermally prepared $CuCo_2O_4$ nanostructure, *Inorganic Chemistry Communications* **170** (2024) 113310. https://doi.org/10.1016/j.inoche.2024.113310

[15] S. Tajik, R. Moghimian, H. Beitollahi, Epirubicin-sensitive detection with a $CoWO_4$/reduced graphene oxide modified screen-printed electrode, *ADMET & DMPK* **13** (2025) 2733. https://doi.org/10.5599/admet.2733

[16] M. Liu, H. Wu, Q. Wang, A multifunctional cucurbit [6] uril-based supramolecular assembly for rifampicin and MnO4− sensing and anti-counterfeiting, *Journal of Molecular Structure* **1318** (2024) 139274. https://doi.org/10.1016/j.molstruc.2024.139274

[17] Z. Fang, M. Ge, W. Jiang, Y. Sun, C. Sun, Microwave-induced Mn (MoO_4) nanosheets on stainless steel mesh enabling high capacity and wide voltage window for supercapacitor applications, *Materials Letters* **417** (2026) 140770. https://doi.org/10.1016/j.matlet.2026.140770

[18] L, Gurusamy, L, Karuppasamy, S, Anandan, C. H. Liu, J. J. Wu, Recent advances on metal molybdate-based electrode materials for supercapacitor application, *Journal of Energy Storage* **79** (2024) 110122. https://doi.org/10.1016/j.est.2023.110122

[19] M. A. Felix, S. S. Shanlee, S. M. Chen, P. Parkavi, C. Ragumoorthy, A. I. Jothi, Conjugated polymer/MnMoO4 hybrid electrode for ultra-trace detection of nilutamide: Toward electrochemical diagnostics in oncology, *Journal of Water Process Engineering* **87** (2026) 110007. https://doi.org/10.1016/j.jwpe.2026.110007

[20] X. Wang, Carbon nanotube-based materials as capacitive deionization electrodes, *New Carbon Materials* **41** (2026) 299-334. https://doi.org/10.1016/S1872-5805(26)61065-7

[21] T. A. Tikish, Y. Worku, N. Palaniyandy, E. E. Ebenso, Recent advances in bimetallic-cobalt oxides and their composites as a potential candidate for supercapacitor electrode material, *Next Energy* **11** (2026) 100505. https://doi.org/10.1016/j.nxener.2025.100505

[22] K. Ahmad, W. Raza, T. H. Oh, Carbon nanotubes-based electrode materials for dopamine sensing and platinum-free dye-sensitized solar cells: A mini review, *Microchemical Journal* **212** (2025) 113352. https://doi.org/10.1016/j.microc.2025.113352

©2026 by the authors; licensee IAPC, Zagreb, Croatia. This article is an open-access article distributed under the terms and conditions of the Creative Commons Attribution license (http://creativecommons.org/licenses/by/4.0/)